Fouling mechanism in dynamic membrane anaerobic bioreactor treating domestic sewage: filtration performance

Jacob Fortuna José Chimuca*, José Tavares de Sousa, Wilton Silva Lopes, Catarina Simone Andrade do Canto, Valderi Duarte Leite

State University of Paraíba (UEPB), Baraúnas Street, 351, University District, Campina Grande, Paraíba, Brazil, CEP: 58429-500, Tel. +55 (83) 3315-3311; email: jacobfortuna66@gmail.com (J.F. José Chimuca)

ABSTRACT

In order to investigate the fouling mechanism in dynamic membrane (DM) formation, and filtration performance in domestic sewage treatment at an ambient temperature ranging from 24°C to 36°C, an anaerobic dynamic membrane bioreactor (AnDMBR) was monitored. Hydraulic retention times applied were 8 and 12 h, under permeate fluxes of 1,755 and 1,170 L m^{-2} h^{-2} in phases I and II, respectively. In both phases, after a 10% reduction in permeate flux, backwashing was performed. This allowed a prolonged filtration of 84 d for phase I and 76 d for phase II. The total resistance to filtration was in the magnitude of 10^{11} m^{-1}, implying excellent filterability by the DM, and energy-saving potential for the AnDMBR system. The system had good treatment performance, achieving average volatile fatty acid reduction of 53%, total chemical oxygen demand (COD) removal efficiencies of 84%, soluble COD of 72%, and color of 80%; being able to remove 94% of suspended solids, and producing an effluent with low turbidity (17 NTU). The biogas measured in the system was 154 N mL g^{-1} COD removed, which represents 35% of its theoretical value, which means that most of it left in dissolved form with the effluent due to supersaturation. The predominant fouling mechanism in DM formation in all permeates fluxes tested was cake filtration, with the main cause being the concentration of inoculum sludge. This confirms the prominence of DM formation during filtration and high solid–liquid separation.

Keywords: Real domestic wastewater; Fouling mechanism; Permeate flux; Total resistance; Filtration performance

1. Introduction

The membrane separation process (MSP) has been studied for a long time as a way to increase efficiency for domestic and industrial wastewater treatment. Potentially, the application of MSP in this field began with synthetic membrane microfiltration (MF) and ultrafiltration (UF) coupled to aerobic and anaerobic bioreactors, having achieved satisfactory results regarding the removal of organic matter and suspended solids [1–5].

However, the main restrictions of MF and UF membranes are related to the high costs, high energy demand, and rapid fouling formation, which cause a significant reduction in permeate flux [6–9]. In extreme situations, the fouling phenomenon is irreversible, causing the membrane performance to not be restored, even after the cleaning step, thus limiting its lifespan [10]. As a consequence, the membranes must be replaced often, bringing more costs to the process [10,11].

A promising alternative for solving problems found in bioreactors with conventional membranes of MF and UF, was the dynamic membrane (DM) technology [12,13]. The DM is also known as a secondary or biological membrane and is usually formed on an underlying support material, which is cheap and has relatively large pores—in the order

---

* Corresponding author.

of 10–200 μm [14–16]. The support material has a low intrinsic resistance (almost negligible) and can be made from mesh, and woven or non-woven filter cloth, when the solution to be filtered contains suspended solids particles such as microbial cells, flocs, and colloids [16].

Despite the economic advantages of DM technology, its stability remains the main concern during practical application. DMs seem to be more applicable in anaerobic bioreactors, taking into account the slow growth of anaerobic microorganisms and the mild hydrodynamic condition due to the absence of aeration [17,18]. The DM, when combined with anaerobic bioreactors, is known as an anaerobic dynamic membrane bioreactor (AnDMBR).

According to Yang et al. [11], Ersahin et al. [18], Siddiqui et al. [19], Ma et al. [20] and Hu et al. [21], with the use of an AnDMBR it is possible to achieve complete biomass retention in the system through the control of cell retention time, regardless of hydraulic retention time. This feature allows the system to treat large volumes in compact treatment units, which allows a longer contact time between the biodegradable material and microorganisms, thus ensuring the removal of the organic material and achieving better sludge stabilization. Thus, it is possible to achieve a treatment efficiency equivalent to that of a conventional MF/UF membrane bioreactor, without the need for high costs.

Guan et al. [16] state that blockage of the support material's pores in DM bioreactor systems is mainly caused by biological flocs, which are mostly bacteria covered by gel-like substances. The blocking of the support material's pores with extracellular polymeric substances (EPS) and soluble microbial products (SMP) is the main fouling factor in MF and UF membrane bioreactors (MBR) [22,23]. This does not occur in AnDMBRs, since the pores are too large to be blocked by EPS and SMP. Wang et al. [15], Saleem et al. [24], and Li et al. [25] state that although there are differences in the way of blocking in the two types of systems, the mathematical modeling systematized by Hermia to elucidate the fouling mechanism in MBRs can also be applied to AnDMBRs.

The mathematical modeling systematized by Hermia consists of four blocking models. The first is the complete blocking model, which assumes that each particle that reaches the surface of the support material clogs a pore. This type of fouling occurs when the solute molecules are larger than the support material pores. The second is the standard blocking model which considers that the obstruction occurs inside the support material pores. This type of fouling is caused by particles smaller than the support material pores. The third, the intermediate blocking model, considers that the pore of the supporting material is not necessarily obstructed by a single particle. This type of fouling occurs when the particles have sizes similar to those of the pores of the supporting material. Finally, in the cake filtration model, the particles are larger than the support material pore size and the concentration of particles is high. The deposition of these particles occurs on the support material surface, forming a layer of particles. Subsequently, a new layer of particles is formed above the first one, and successively thereafter [24–26].

Until now, however, studies have only addressed the mechanism of DM formation using the mathematical modeling systematized by Hermia in the treatment of synthetic wastewater in the AnDMBR system. From this perspective, this study intends to investigate the applicability of the mathematical modeling systematized by Hermia in the treatment of real domestic wastewater by an AnDMBR on a pilot scale, at ambient temperature, in order to understand the main mechanisms that govern the DM layer formation and evaluate the possible effects of the variation of operational parameters on DM development and performance.

2. Material and method

2.1. Experiment location and the capture of domestic sewage

The experimental system was built and monitored at the Experimental Station of Biological Treatment of Sanitary Sewage (EXTRABES), located in the municipality of Campina Grande, in the state of Paraíba, Brazil, at an altitude of 550 m, with an ambient temperature that ranged from 22°C to 36°C, at the geographical coordinates 7°, 14′, 23.26′ S and 35°, 53′, 03.23′ W.

The sewage used during the experimental period came from a housing development (HD) with 72 apartments, located 200 m from the EXTRABES area, with an average flow rate of 20 m³ d⁻¹. The average raw chemical oxygen demand (COD) concentration was 958 mg COD L⁻¹; strong sewage, according to Metcalf & Eddy [27]. The description of the domestic sewage used in this study is presented in Table 1.

2.2. Experimental system description

The experimental AnDMBR system consisted of an anaerobic bioreactor and an external membrane module for filtration (Fig. 1). The bioreactor was built from fiberglass and the membrane module from polyvinyl chloride (PVC). The support material for the formation of the dynamic membrane was polypropylene. Below the polypropylene mesh, a stainless steel mesh was used to provide a frame and structuring to the layer under the support material when subjected to high internal pressure. The dimensions of the anaerobic bioreactor and the membrane module are presented in Table S1.

Transmembrane pressure (TMP) was monitored daily by MPX4250 pressure sensors installed in the inlet and outlet line of the membrane module to monitor the behavior and formation of the dynamic membrane, as well as to evaluate physical and chemical characteristics. The sensors were connected to an Arduino Uno ATmega328 microcontroller board, responsible for the communication between the bioreactor and the computer. The pressure values were provided by the SisMonBio software through spreadsheets generated every 5 min and stored in the system. The software recorded and displayed information in real-time, and also made it possible to consult data from the bioreactor according to the desired date.

The biogas produced was quantified by measuring the pressures accumulated in the headspace throughout the days of operation, using the biogas pressure sensor, and visualized through the SisMonBio software developed by Ramos et al. [29]. The daily quantified pressures

were transformed into biogas volume under normal temperature and pressure conditions (NTP) according to the law of gases. The methane COD was calculated based on Eq. (1). The theoretical methane production was estimated by applying Eqs. (2) and (3).

$$COD_{CH_4} = Q(S_0 - S) - Y_{obs} \cdot Q \cdot S_0 \tag{1}$$

where COD_{CH_4} is the load converted into methane $\left(kg\ COD_{CH_4}\ d^{-1}\right)$; Q is the influent sewage flow (m³ d⁻¹); S_0 and S are the COD concentration (kg COD m⁻³) of influent and effluent, respectively; and Y_{obs} is the coefficient of production of solids in the system, in terms of COD (0.11 to 0.23 kg COD_{sludge} kg⁻¹ $COD_{applied}$).

$$Q_{CH_4} = 22.4 \frac{L}{mol} \left(\frac{273,15 + t}{273,15} \right) \frac{COD_{CH_4}}{64\ g\ COD\ mol^{-1}\ CH_4} \tag{2}$$

where Q_{CH_4} is the estimated volumetric methane production (m³ d⁻¹); t is the temperature under NTP equal to 0°C.

$$Q_{biogas} = \frac{Q_{CH_4}}{\%C_{CH_4}} \tag{3}$$

where Q_{biogas} is the volumetric production of biogas quantified in the system (m³ d⁻¹); Q_{CH_4} is the estimated volumetric methane production (m³ d⁻¹); C_{CH_4} is the methane content (%) in biogas which was 70%, used because van Haandel and Lettinga [30], Chernicharo [31] and Hu et al. [32] state that the methane content in the anaerobic treatment of domestic sewage generally varies from 70% to 80%.

2.3. Monitoring of the experimental system

The AnDMBR system was started in January 2020. The system feeding process was carried out continuously and under constant flow with the assistance of an R Line Helical Gear Motor (Sew-Eurodrive, model NM008BY03S12B, Brazil). The effluent coming from the anaerobic digester was routed by hydraulic pressure (as a driving force) to the membrane module. After passing through the dynamic membrane, the effluent (permeate) flowed by gravity into a collection container. The filtration was performed by transverse flux (perpendicular), under two different initial permeate fluxes (J_p) called phase I (J_p = 1,754.8 L m⁻² h⁻¹) and phase II (J_p = 1,169.9 L m⁻² h⁻¹). Details of operational parameters are found in Table S1.

Phase I started with inoculum (21 g VSS L⁻¹ and 15 L = 315 g VSS) from the UASB reactor, while phase II started with inoculum (28.7 g VSS L⁻¹ and 15 L = 430.5 g VSS) from the same AnDMBR system—immediately after completion and removal of the phase I excess sludge (Table 2). System operation times for phases I and II were 84 and 76 d, respectively. During system operation, after a 10% reduction in permeate flux, backwashing was performed. In backwashing with effluent from the bioreactor, taps 1 and 3 were closed while taps 2 and 4 were opened for reverse flow, as shown in Fig. 1. The re-washing time was 1 min, which was sufficient for an average output volume of 0.12 L d⁻¹ of the concentrated solution by tap 2, with an average COD of 51.8 g L⁻¹ for phase I and 10.5 g L⁻¹ for phase II, producing 6.218 g COD d⁻¹ and 1.244 g COD d⁻¹, respectively.

2.4. Analytical methods

Daily, weekly, and fortnightly analyses were performed to characterize the AnDMBR affluent and permeate. It should be noted that the samples used for the analysis of soluble COD and suspended solids was centrifuged at a rotation of 6,000 rpm, for 15 min.

Sludge from the bioreactor, from backwashing, and from the DM were also characterized. Sludge flocculability

Table 1
Physiochemical and biological characteristics of phases I and II influent

Parameter	Phase I	Phase II
	Average values ± SD	Average values ± SD
COD, mg L⁻¹	967.5 ± 37.8	933.4 ± 40.2
CODs, mg L⁻¹	275.0 ± 7.8	284.5 ± 12.3
Color	44.0 ± 2.9	41.4 ± 4.4
Helminth eggs, egg L⁻¹	29.8 ± 3.2	31.1 ± 1.7
Carbohydrates, mg L⁻¹	23.2 ± 0.8	22.6 ± 1.17
Proteins, mg L⁻¹	44.0 ± 2.2	42.2 ± 2.1
Turbidity, NTU	359.5 ± 37.1	388.8 ± 32.3
TSS, mg L⁻¹	476.9 ± 19.1	458.1 ± 25.4
VSS, mg L⁻¹	344.2 ± 16.8	332.2 ± 5.9
TKN, mg L⁻¹	83.5 ± 1.6	82.86 ± 1.06
TP, mg L⁻¹	14.26 ± 1.45	13.84 ± 0.47
VFAs, mg L⁻¹	87.67 ± 2.77	88.0 ± 3.35
pH	7.2	7.3

COD: chemical oxygen demand; CODs: soluble chemical oxygen demand; TSS: total suspended solids; VSS: volatile suspended solids; TP: total phosphorus; TKN: total Kjeldahl nitrogen; VFAs: volatile fatty acids.
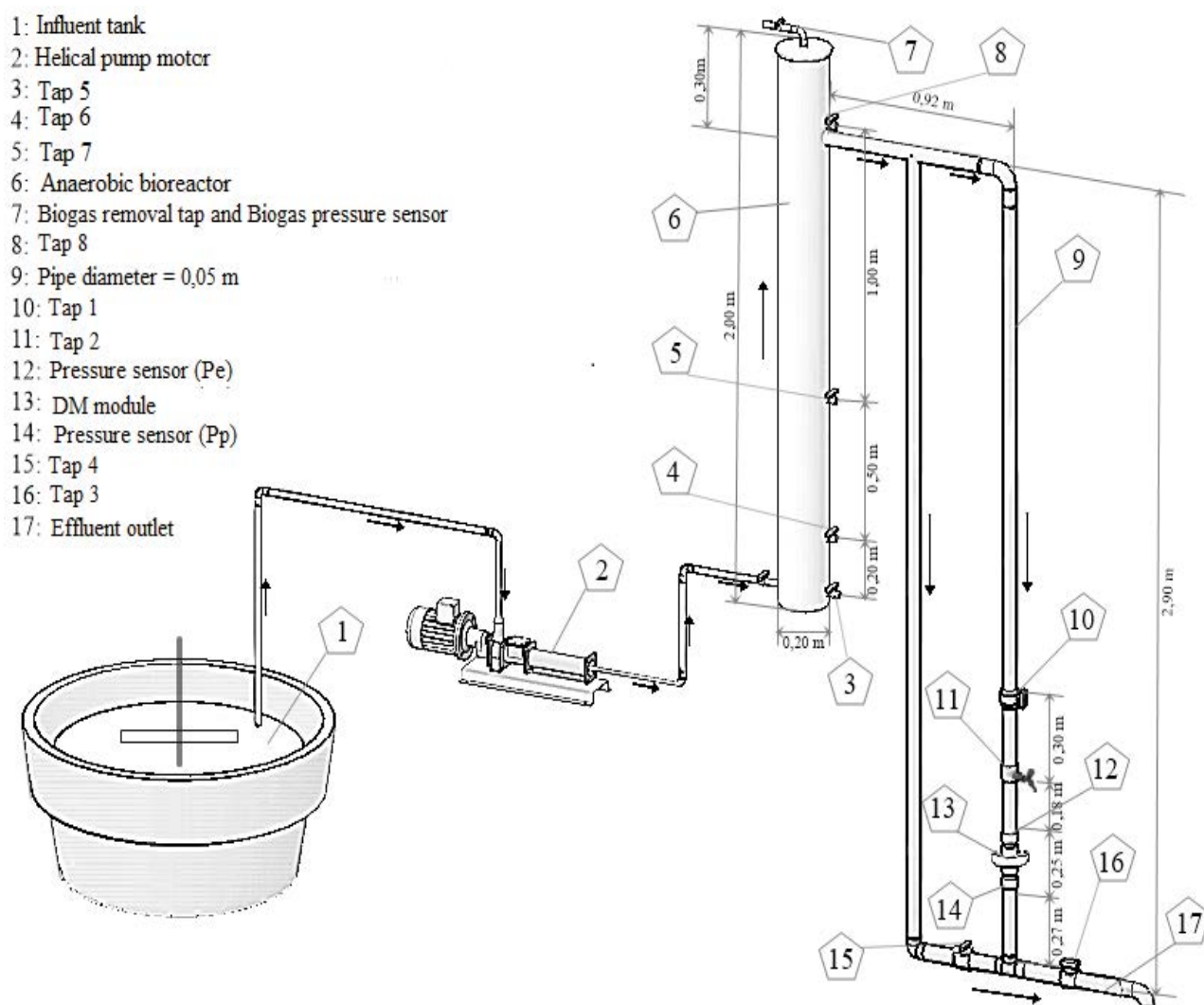
1: Influent tank
2: Helical pump motor
3: Tap 5
4: Tap 6
5: Tap 7
6: Anaerobic bioreactor
7: Biogas removal tap and Biogas pressure sensor
8: Tap 8
9: Pipe diameter = 0,05 m
10: Tap 1
11: Tap 2
12: Pressure sensor (Pe)
13: DM module
14: Pressure sensor (Pp)
15: Tap 4
16: Tap 3
17: Effluent outlet

Fig. 1. Schematic drawing of the experimental system.

Table 2
Characterization of inoculum sludge from phases I and II

Parameter	Phase I	Phase II
	Values	Values
pH	7.3	7.6
Sludge volume index (SVI), mg L^{-1}	28	31.5
Supernatant turbidity, NTU	220.3	211.3
TSS, g L^{-1}	30.9	43.3
VSS, g L^{-1}	21	28.7
COD, g L^{-1}	25.62	37.3
CODs, g L^{-1}	0.155	0.16
TKN, g L^{-1}	0.36	1.79
Total phosphorus, g L^{-1}	0.17	0.95
Carbohydrates, mg g^{-1} VSS	14.7	18.1
Proteins, mg g^{-1} VSS	23.8	31.3
Proteins/Carbohydrates (PN/PS)	1.62	1.73

was determined by supernatant turbidity, measured with a turbidity meter (MS Tecnopon, model TB-1000P, Brazil) after 30 min of sedimentation.

Physical and chemical analyses followed the Standard Methods for the Examination of Water and Wastewater [33] recommendations. Helminth eggs followed modified BAILENGER methodology [34].

SMP concentrations were measured as proteins and carbohydrates. For this purpose, the collected samples were centrifuged for 30 min at 6,000 rpm and the extracted supernatant was filtered through a 0.45 μm membrane. The centrifuged supernatant filtrate was denominated as SMP. Proteins were measured using the Lowry method modified by Frøund [35], with the BSA standard (Bovine Serum Albumin, Sigma V fraction, 96%). Carbohydrates were measured using the method described by Dubois et al. [36] with a glucose pattern.

The effluent (permeate) viscosity was measured with a rotary viscometer (microprocessed, model Q860M26, Brazil). The total filtration resistance was calculated based on Eq. (4).

$$R_T = \frac{\text{TMP}}{\mu \cdot J_P} \tag{4}$$

where R_T is the total filtration resistance (m^{-1}); TMP is the transmembrane pressure (Pa); μ is the effluent viscosity (Pa·s); J_P is the permeate flux (m^3 m^{-2} s).

2.5. Mass balance of the AnDMBR system

The quantification of organic matter fractions expressed in COD form present in the effluent, in excess sludge, the DM, and in the methanized fraction was estimated with the mass balance from Eq. (5). The same equation was used for nutrients.
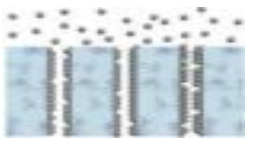
$$M_A + M_I = M_{\text{LE}} + M_P + M_T + M_B + M_C \tag{5}$$

where M_A is the daily mass of feed; M_I is the daily mass of inoculum; M_B is the daily mass converted to methane; M_{LE} is the daily mass of backwashing sludge; M_P is the daily mass of effluent; M_T is the daily mass of dynamic membrane; M_C is the daily mass of bioreactor sludge.

2.6. Data analysis

With the help of the IBM SPSS 25 statistics software, correlation analysis was performed using p-value and Pearson correlation coefficients (r_p). Pearson correlation (r_p) and regression (R^2) coefficients were used to provide an indication of the linear correlation between permeate flux, PTM, resistance to filtration and effluent turbidity. Unilateral variance analysis (ANOVA) of the parameters related to treatment efficiency was performed, and the level of significance was established at 5%, p-value > 5%, and p-value < 5%, corresponding to no significant difference and significant difference between treatments (phases), respectively.

For the mathematical modeling analysis of the fouling mechanism in DM formation, the TMP experimental data were processed in OriginPro 2018. The equations of the Hermia model and schematic representation (Table 3) extracted from Wang et al. [15] and Iritani & Katagiri [26]—complete blocking, standard blocking, intermediate blocking, and cake filtration—were inserted as user-defined functions in Origin software. TMP data were adjusted with data from the automatic models. The constants of each model (K_b, K_s, K_i, and K_c, respectively), the residual sum of squares (RSS), and the adjusted coefficient of determination (R^2_{adj}) were obtained during analysis using the software. According to Li et al. [25], the adjusted R^2_{adj} indicates the proportion of experimental TMP data predictable from time in the analysis of the DM formation mechanism; the RSS represents the error between the experimental, and the model predicted TMP data.

3. Results and discussion

3.1. Transmembrane pressure behavior, total filtration resistance, and permeate flux.

Fig. 2 shows the behaviors of TMP and total resistance to filtration over time, obtained for phases I and II of the AnDMBR system.

In both phases, TMP increased progressively throughout most of the operating time (Fig. 2). In phase I, TMP reached the maximum value of 47.6 kPa at 85 d, being that after 52 d it had a gradual increase, with an average of 45.6 ± 2.0 kPa, indicating that it was the maturation stage. From day 76 until the end of the operation period, there was a lot of oscillation, suggesting the occurrence of the breaking and dissociation stage of the DM layer. Wang et al. [15] state that the process of DM formation can occur in three stages: DM layer formation, clogging or compression, and dissociation. This is confirmed in the study by Guan et al.

Table 3
Mathematical modeling to assess the evolution of fouling over time

Filtration model	Model equation	Blocking constant	Schematic representation
Complete blocking	$\dfrac{P}{P_0} = \dfrac{1}{1 - K_b \cdot t}$	K_b (1 s^{-1})	
Standard blocking	$\dfrac{P}{P_0} = \left(1 - \dfrac{K_s \cdot J_0 \cdot t}{2}\right)^{-2}$	K_s (1 m^{-3})	
Intermediate blocking	$\dfrac{P}{P_0} = \exp\left(K_i \cdot J_0 \cdot t\right)$	K_i (1 m^{-3})	

P is TMP (Pa); P_0 is initial TMP (Pa); J_0 is flow (L h^{-1}); K_b is complete blocking constant; K_s is standard blocking constant; K_i is intermediate blocking constant; K_c is cake filtration constant.
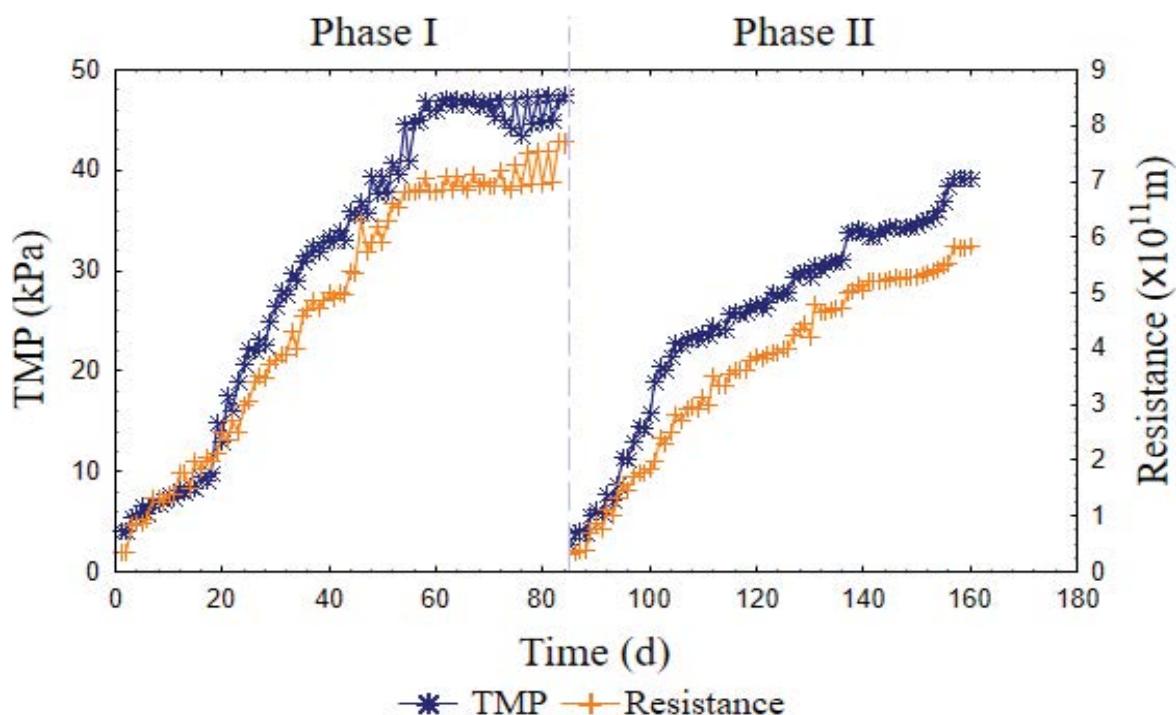
Fig. 2. TMP behavior and total resistance to filtration in phases I and II during operating time.

[37], which observed the dissociation of the DM layer when TMP reached values above 40 kPa. In phase II, the maximum TMP was 39.3 kPa at 73 d. After 50 d there was little variation in the gradual increase in the curve, with an average of 35.4 ± 2.0 kPa, indicating the maturation stage.

TMP average values for each period of operation for phases I and II were 30.7 ± 15.3 and 25.3 ± 10.2 kPa, with an increased rate of 0.37 and 0.32 kPa d^{-1}, respectively. Phase I had an average value and TMP increase rate higher than phase II. This can be explained by the higher amounts of SMP proteins and carbohydrates accumulated in the DM layer (Table 4), probably coming from the reactor's liquid phase, due to relatively short hydraulic retention time (HRT) (Table S1). In addition, it was found that the protein/carbohydrate ratio (PN/PS) was also higher in phase I, implying a greater accumulation of protein in relation to carbohydrates. Hu et al. [32], Ersahin et al. [38] and Shi et al. [39] state that greater accumulation of SMP in the DM, especially proteins, leads to high values of TMP and resistance to filtration.

However, the high value of TMP in phase I of this study may be explained by high initial permeate flux. It also may be influenced by surface velocity (Table S1). Siddiqui et al. [19] stated in their study that high initial flows resulted in high TMP values, when compared to low initial flows. Similar results were observed by Yang et al. [11] for an AnDMBR when they evaluated four HRTs under permeate variation flow. The authors explained this fact by the flow velocity—which was much higher for the short HRT and high flows—causing washing of fine particles in the beginning, and the retention of large particles with good sedimentation capacity, thus increasing the TMP. These aspects

Table 4
SMP composition in DM layer for phases I and II

	Phase I	Phase II
Carbohydrates (mg g^{-1} VSS)	118.7	75.2
Proteins (mg g^{-1} VSS)	244.0	120.4
PN/PS	2.06	1.60

are ratified and supported by Sun et al. [40] on the fundamentals of fluid mechanics for the formation of the DM.

Analogous to the TMP behavior, in the present study a filtration resistance was also observed, ranging from 0.36–7.6 × 10^{11} m^{-1} in phase I, and 0.32–5.84 × 10^{11} m^{-1} in phase II (Fig. 2). The average filtration resistance during all operating time for phase I was 4.9 ± 2.3 m^{-1}, and 3.7 ± 1.6 m^{-1} for phase II. Although the filtration resistance showed variation throughout the operational period of each phase, the values were 10^{11} m^{-1}, implying excellent filterability by the DM and great potential for energy savings with the AnDMBR system. This magnitude is much lower than the one obtained in the filtration process by conventional MF/UF membranes, which range from 10^{12} to 10^{14} m^{-1} according to Lin et al. [41], Hao et al. [42] and Zhu et al. [43]. These authors claim that a magnitude from 10^{12} to 10^{14} m^{-1} requires much more driving force to overcome resistance to filtration during permeation.

Similar results were achieved by Liu et al. [44] in the AnDMBR. They verified filtration resistance values ranging from 1.0 to 3.0 × 10^{11} m^{-1}, during about 70 d of the stable operation stage. They also explained that filtration

resistance can be maintained at low levels in stable operation stages with a single cleaning of the membrane.

The permeate flux behavior during the operating time in all phases is shown in Fig. 3.

Fig. 3 shows that the permeate flux of all phases decreased over the system operation period. There was little variation in the flow in the first 3 d of operation. In the same period, TMP increased from 4.2 to 5.5 kPa in phase I, and 2.7 to 4.0 kPa in phase II. From the fifth day there was a reduction of approximately 10% in the permeate flux for both phases, in which TMP reached values of 6.5 kPa in phase I and 5.6 kPa in phase II. Similar results were observed by Chimuca et al. [28] when operating the same system in a single-phase divided into two cycles; without backwashing (Cycle 1), and with backwashing (Cycle 2), under an initial permeate flux of 780 L m^{-2} h^{-1}.

The low variability in the permeate flux for the first days of operation, which occurred in all phases in the present study, can be explained by the low flocculability of the inoculum sludge (indicated by the high turbidity of the supernatant) as shown in Table 2. The low flocculability of the sludge probably affected the onset of DM formation, and consequently, the decrease in permeate flux. This may have occurred due to the sludge flocs that were deposited on the surface of the support mesh, exerting pressure on it, and consequently increasing the TMP. However, the sludge flocs took a long time to adhere to the support mesh, and therefore, to initiate the DM layer formation which did not allow a significant reduction of permeate flux or effluent turbidity (Fig. 4). This is confirmed by Hu et al. [45] and Yu et al. [46], who state that permeate flux can maintain high values for a long period of operation (3–5 d) under TMP variation.

Therefore, even with the application of backwashing in both phases, the permeate flux continued to decrease and the TMP increased significantly (p-value = 0.000) over the operating time, as evidenced by the Pearson linear correlation coefficients (r_p), presented in Table 5. The r_p between permeate flux and TMP varied between –0.865 and –0.970, being classified as a strong negative correlation. A similar result also occurred between permeate flux and filtration resistance (r_p = –0.878 to –0.976). Alibardi et al. [47] verified similar behavior for TMP and permeate flux in their AnDMBR system from 90 d of operation. The researchers justified this fact based on Darcy's law, which confirms the development of a stable DM when there is approximate proportionality between a system's permeate flux and TMP.

In this sense, it was found that there was more stability in the DM development in phase II than in phase I, since the regression coefficient between permeate flux and TMP was higher in phase II ($R^2 = 0.960$) than in phase I ($R^2 = 0.747$).

3.2. Performance of the AnDMBR system in the treatment of domestic sewage

The turbidity values for the influent and effluent during the operating time in all phases are shown in Fig. 4.

According to the data in Fig. 4, in phase I a considerable reduction in the effluent turbidity was from observed day 36, when the lowest value of 31 NTU was reached, with maximum efficiency of 90.2%. In the stationary period, the average value was 56 ± 34.9 NTU. In phase II, a considerable reduction began to be recorded from day 18 of operation, reaching the lowest value of 17.3 NTU at 73 d. In the stationary period, the average value was 33.8 ± 27.2 NTU. However, it is observed that in both phases the turbidity
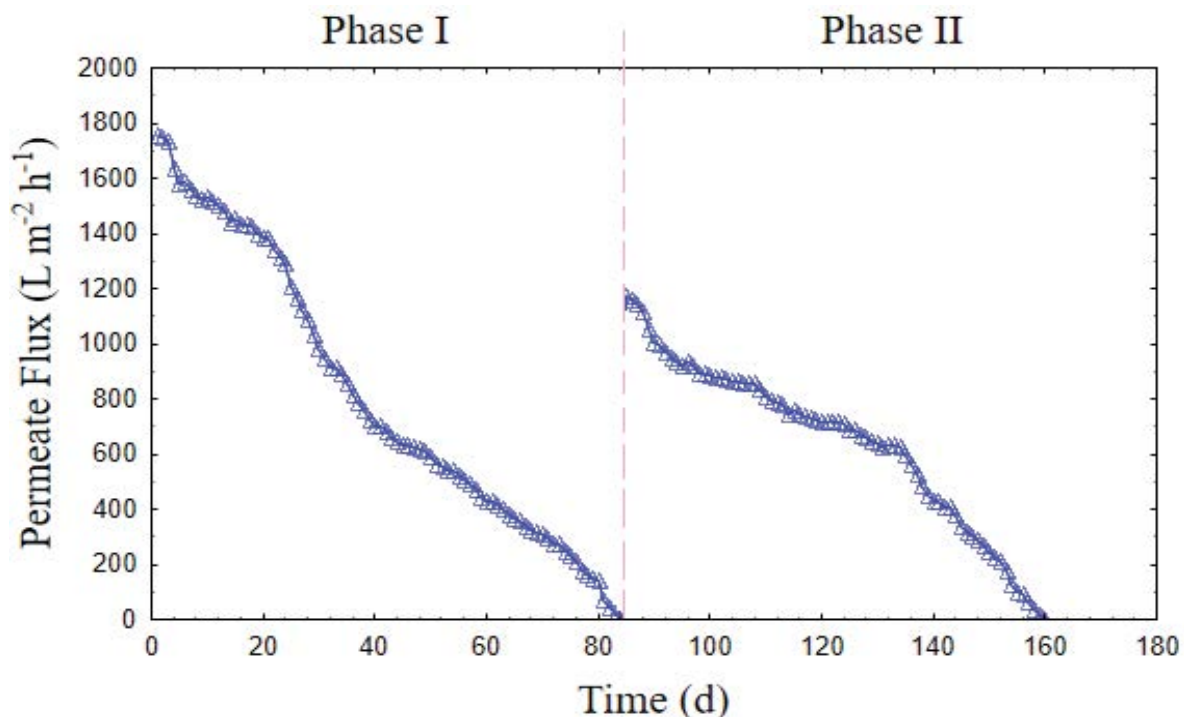

Fig. 3. Permeate flux profile in phases I and II during operating time.
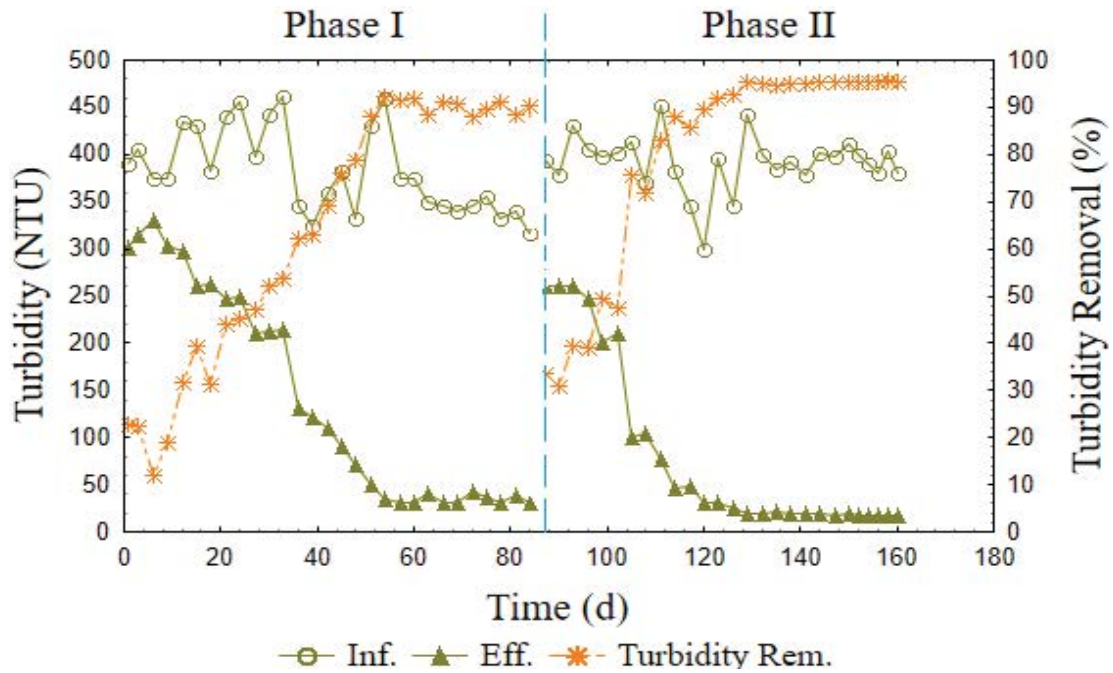
Fig. 4. Turbidity variation in phases I and II during system operation time.

Table 5
Permeate flux ratio, TMP, filtration resistance, and effluent turbidity

Experiment	Control variable	Factor	Coefficients and p-value	TMP	Filtration resistance	Effluent turbidity
Phase I			r_p	−0.865	−0.878	0.804
			p-value	0.000	0.000	0.000
			R^2	0.747	0.869	0.633
	Time	Permeate flux	p-value	0.000	0.000	0.000
			r_p	−0.970	−0.976	0.933
Phase II			p-value	0.000	0.000	0.000
			R^2	0.960	0.971	0.865
			p-value	0.000	0.000	0.000

was extremely high in the first 9 d of operation, due to the fact that the DM had not yet been developed.

On the other hand, the correlation between permeate flux and effluent turbidity was significant (p-value = 0.000) in both phases, with r_p values between 0.804 and 0.933, being classified as strong positive correlation. This means that as the permeate flux decreases, the effluent turbidity also decreases. As for stability, Table 5 shows that the regression coefficient between permeate flux and turbidity in phase I was the lowest (R^2 = 0.63). This may be associated with the high initial value of the permeate flux that had a negative impact (high TMP) on the maturation stage of the DM layer, causing dissociation of the DM layer and elution of the biological flocs, associated with high TMP values (as discussed previously), thus causing a significant increase in effluent turbidity. Pollice and Vergine [48] ratify this fact, explaining that the permeate flux clearly influences DM development. DM fouling is more intense for very high flow values, and there is deterioration of effluent quality.

Yang et al. [11] observed a significant reduction in filtration performance due to the turbulence which occurred in the DM when they operated the AnDMBR system under high permeate flux values and short HRT.

However, even with statistically different effluent turbidity between phases (ANOVA with p-value = 0.0012) in the present study, the average values obtained are similar to those obtained by Hu et al. [32] in the study on domestic wastewater treatment. Operating under a flow of 22.5 L m^{-2} h^{-1}, they verified a turbidity variation between 30 and 50 NTU in the effluent. These values were attributed to the effective retention of particulate substances by the stable DM layer.

Volatile fatty acid (VFA) values for the influent and effluent during the operating time in all phases are shown in Fig. 5.

Fig. 5 shows VFA reduction in the stationary period in phase I, corresponding to 48.4%. In phase II, the reduction was 57.3%. The ANOVA showed a significant difference in
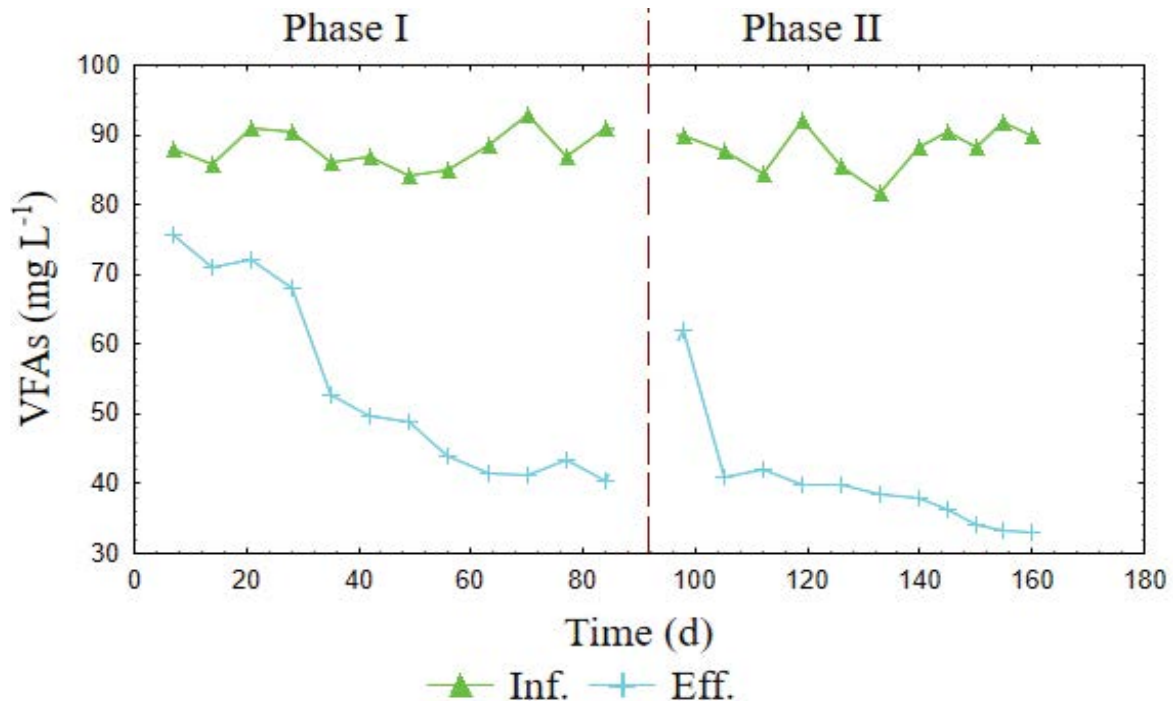
Fig. 5. Average VFA values throughout system operation period (phases I and II).

VFA reduction between the phases (p-value = 0.0042), which suggests that the methanogenic activity was more intense in the DM layer in phase II. Ershain et al. [18] obtained a 50% reduction in VFA concentrations in both the AnDMBR external module system and the AnDMBR submerged module system. The authors attributed the greatest reduction to the DM formed in the stationary period in both systems. Yang et al. [11] observed a reduction between 20% and 45% of VFA removal by the AnDMBR system in domestic wastewater treatment.

Liu et al. [49] state that the application of a DM increases AnDMBR substrate retention capacity, subsequently stimulating the alteration of the dominant microorganisms. This is since there is an increase in the amount of hydrolytic enzymes such as protease and β-glycosidase, resulting in changes in the organic matter degradation pathways. In addition, bacteria that are essential for refractory organic matter degradation—which normally exhibit low growth rate—are retained by the DM layer and accumulated, resulting in a greater degradation of refractory substances for conversion into by-products such as VFAs.

The concentration values of total COD (COD) and soluble COD (CODs) of the affluent and effluent during the operating time of the AnDMBR System (phases I and II) are shown in Fig. 6.

Fig. 6a shows that the maximum efficiency for total COD removal in phase I was 80.9% at 77 d, and the average in the stationary period was 78.6% ± 1.9%. In phase II, the maximum efficiency for total COD was 88.1% at 76 d, and the average was 86.4% ± 0.8%. As for the removal of the soluble COD (Fig. 6b), in phase I the maximum efficiency was 64.5% at 77 d, and the average in the stationary period was 59.6% ± 3.8%. In phase II, the maximum efficiency was 79.0% at 76 d, and the average was 74.6% ± 2.7%.

ANOVA showed a significant difference in total and soluble COD between the phases (p-value = 0.021). Therefore, it can be stated that the AnDMBR system had good removal of total and soluble COD in both phases. These values are similar to those obtained by several authors with the AnDMBR system, such as Yang et al. [11], who obtained removal efficiencies of 74.4%, 77.3%, 70.6%, and 60.4% under permeate fluxes of 22.5, 45, 90, and 180 L m^{-2} h^{-1}, respectively. Paçal et al. [50] achieved total COD removal efficiencies between 75% ± 6% and 86% ± 12%. Hu et al. [32] achieved total COD removal efficiencies between 70% and 90%, and for soluble COD from 54% to 70% under 22.5 L m^{-2} h^{-1}. This achieved a total COD removal efficiency which was rated as high. Wang et al. [51] obtained total COD removal efficiency of 80%, in an AnDMBR system at different permeate fluxes (50, 100, and 150 L m^{-2} h^{-1}).

3.2.1. Other AnDMBR system performance parameters

Fig. S1 shows that the stabilization of solids in the effluent at all stages presented the same behavior regarding turbidity. In the stationary period, total suspended solids (TSS) and volatile suspended solids (VSS) effluent concentrations ranged from 79 to 113 mg L^{-1}, and from 66.4 to 91 mg L^{-1}, respectively, in phase I. In phase II, effluent TSS and VSS concentrations ranged from 31 to 77 mg L^{-1} and from 22.6 to 40.4 mg L^{-1}, respectively. Similar results were found by Ma et al. [20], Alibardi et al. [14], Alibardi et al. [47], Paçal et al. [50] and Berkessa et al. [52].

In both phases, a decrease in the concentration of helminth eggs in the effluent was observed (Fig. S2). The average concentration of helminth eggs in the effluent during the stationary period was 0.73 ± 0.67 L^{-1} eggs for phase I,
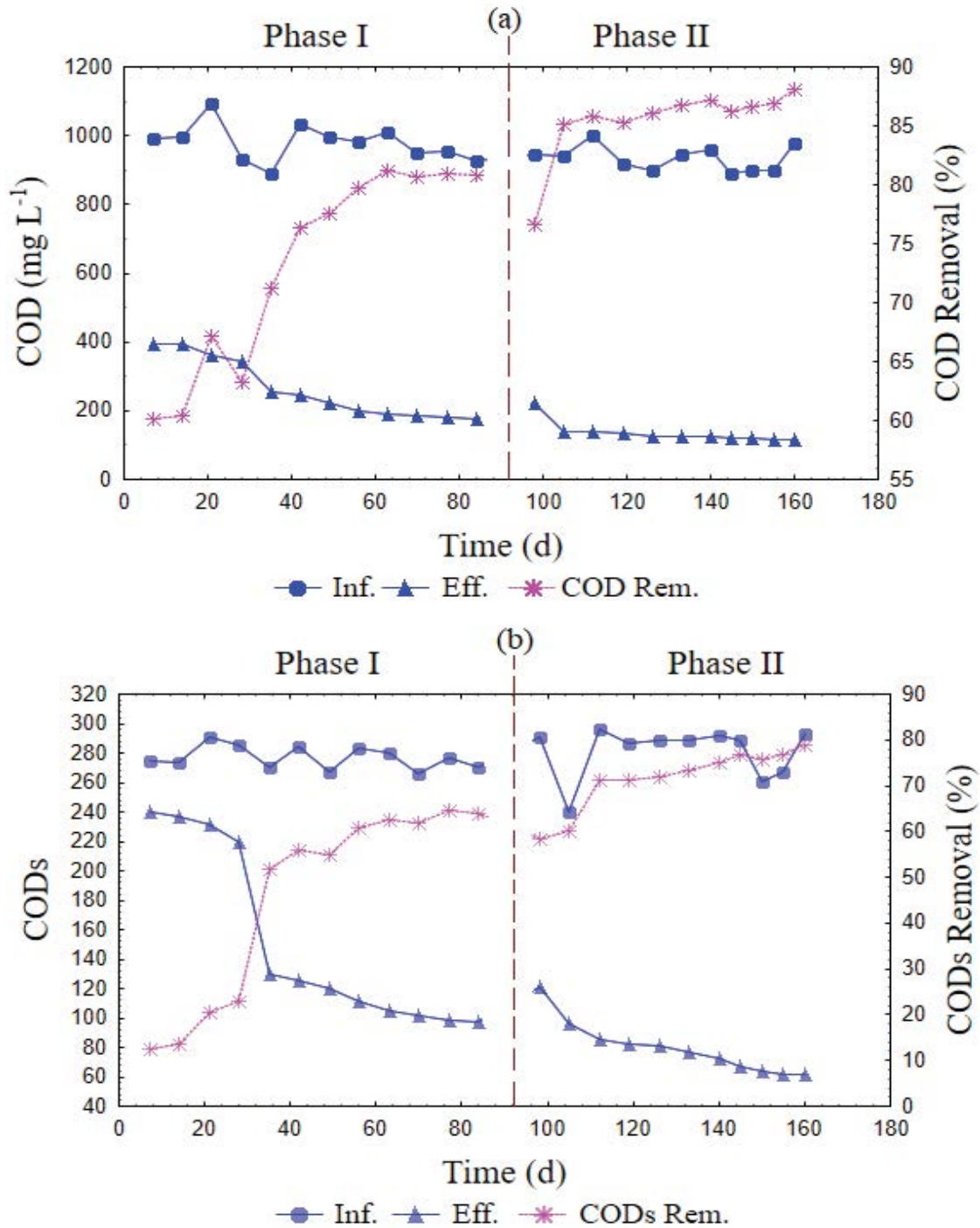
Fig. 6. Variation of total and soluble COD concentration during system operation time, phases I and II.

and 0.44 ± 0.57 L^{-1} eggs for phase II. Therefore, ANOVA showed an insignificant difference in the average concentration of helminth eggs between phases. *Ascaris lumbricoides* was predominant in both the influent and the effluent (Table S2). Similar results were obtained by Chimuca et al. [28]. As for color, Fig. S3 shows that the removal efficiency reached 63.3% at 84 d in phase I and 80% at 76 d in phase II. Similar values were found by Yu et al. [53].

3.3. Biogas production

Fig. 7 shows the quantified biogas production behavior in all phases. Phase I average production was 149.1 ± 36.7 N mL g^{-1} COD removed, and in phase II, 158.5 ± 41.3 N mL g^{-1} COD removed, corresponding to volumetric production of 18.3 ± 5.2 LN d^{-1} and 13.4 ± 3.5 LN d^{-1}, respectively.
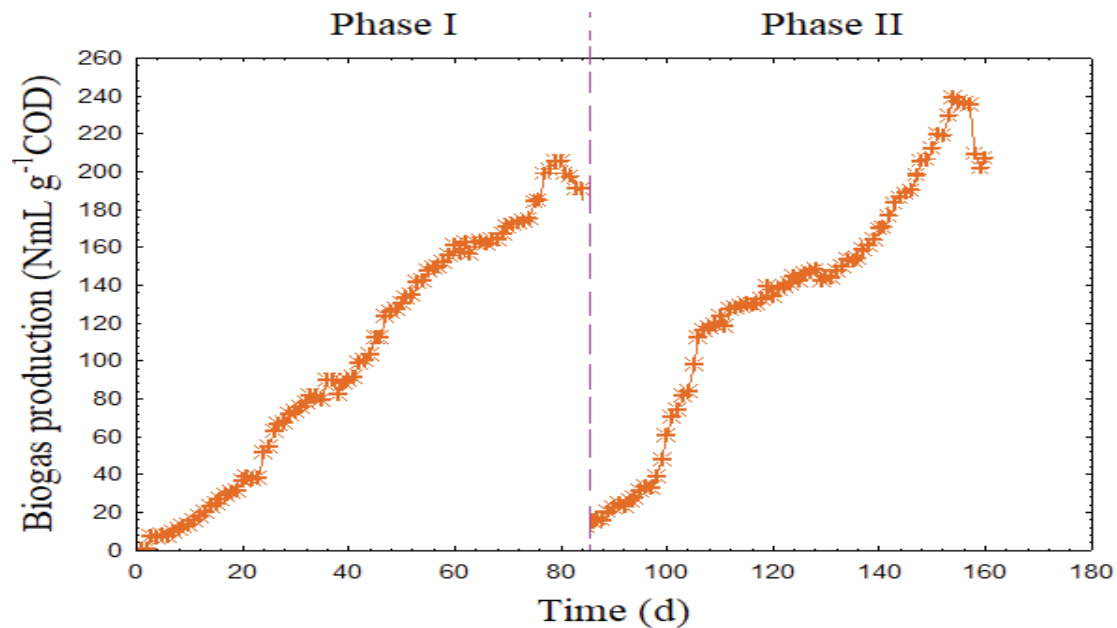
Fig. 7. Biogas production behaviour during operation of phases I and II.

According to van Haandel and Lettinga [30], Chernicharo [31], and Hu et al. [32], methane levels in biogas are generally in the order of 70%–80% in domestic wastewater treatment by anaerobic digestion. With this in mind, considering that 70% of the biogas is in the form of methane, the methane yields for phases I and II were 104.37 and 111 mLNCH$_4$ g^{-1} COD removed, respectively. ANOVA showed an insignificant difference in biogas production between the phases (*p*-value = 0.681).

The theoretical values of estimated biogas, based on Eqs. (2) and (3), were 435 NmL g^{-1} COD removed for phase I, and 434.6 NmL g^{-1} COD removed for phase II. It is suggested that the quantified biogas production for phases I and II represents only 34.3% and 36.5% of the theoretical values, respectively.

It is observed that the biogas production and the average methane yield in both phases were much lower than the theoretical values. This can be explained by the considerable output of biogas in dissolved form with effluent from the system. Pauss et al. [54] stated that the liquid-gas mass transfer coefficient changes significantly according to the reactor configuration and operating conditions. It can lead to methane concentrations in the liquid phase that are up to 12 times higher than the equilibrium values.

It is understood that the low value of methane yields obtained was due to a real concentration of methane dissolved in the liquid phase, which is considerably higher than the amount calculated under thermodynamic equilibrium. This hypothesis is confirmed by Hu et al. [21], Hu et al. [55], Yang et al. [11], Ersahin et al. [56], and Paçal et al. [50].

3.4. AnDMBR mass balance

To evaluate the process efficiency, a daily mass balance was performed in the stationary period, based on the average loads of the following parameters: total COD, total

Kjeldahl nitrogen (TKN), and total phosphorus; whose values are presented in Table 6. The total COD balance fraction behaviors are presented in detail in Fig. 8.

Fig. 8 shows that in phases I and II, the carbonaceous material of the effluent represented, respectively, 21% and 13% of the total that entered the system. Of this fraction, most of it came out in soluble form. Similar results were observed in other AnDMBR studies. In the study by Chimuca et al. [28], under a flow of 780 L m^{-2} h^{-1}, values of 12% operating with backwashing, and 14% without backwashing were obtained. Alibardi et al. [47] found values between 11% and 25% when under three distinct HRTs (2, 1, and 0.5 d).

In Table 6 it is noted that the produced sludge total was 25.81 gCOD d^{-1} for phase I and 19.48 gCOD d^{-1} for phase II, representing 84.2% and 94.8% of the theoretical sludge production of 30.65 gCOD d^{-1} and 20.55 gCOD d^{-1}, respectively. The difference between the produced sludge COD value and the theoretical sludge COD value was considerable for phase I (15.8%) and not considerable for phase II (5.2%). The considerable difference in phase I can be explained by the biological flocs' elution to the effluent, due to the dissociation of the DM layer from 76 d until the end of the operation period, as discussed in subchapter 3.1.

However, although in phase II there was considerable difference between the values of produced COD and theoretical sludge COD, the sludge production coefficients were 16% for phase I and 18% for phase II (Fig. 8). These values are within the ranges of 11% to 23% presented by van Haandel and Letiinga [30], and Chernicharo [31]. COD fractions of 63% and 69% converted in phases I and II, respectively, are close to the maximum values of 70% mentioned by van Lier et al. [57].

Table 6 also shows the values of TKN and total phosphorus. Through the mass balance, TKN removal efficiencies of 18.9% for phase I and 21.2% for phase II were

Table 6
Daily total COD mass balance, TKN, and total phosphorus for phases I and II

|		COD (g d⁻¹)		TKN (g d⁻¹)		Phosphorus (g d⁻¹)	
		Phase I	Phase II	Phase I	Phase II	Phase I	Phase II
Entry	Influent	156.732	100.803	13.541	8.949	4.089	1.495
	Inoculum	4.575	7.367	0.064	0.354	0.030	0.187
	Total	161.307	108.170	13.605	9.303	4.119	1.682
	Effluent	33.875	14.063	10.984	7.052	3.458	1.230
	DM	7.144	7.896	0.406	0.475	0.220	0.127
	Backwashing	6.218	1.254	0.095	0.091	0.041	0.037
Output	Bioreactor	12.443	10.329	0.597	0.796	0.317	0.263
	Methane	101.627	74.628		–	–	–
	Total	161.307	108.170	12.802	8.414	4.036	1.657
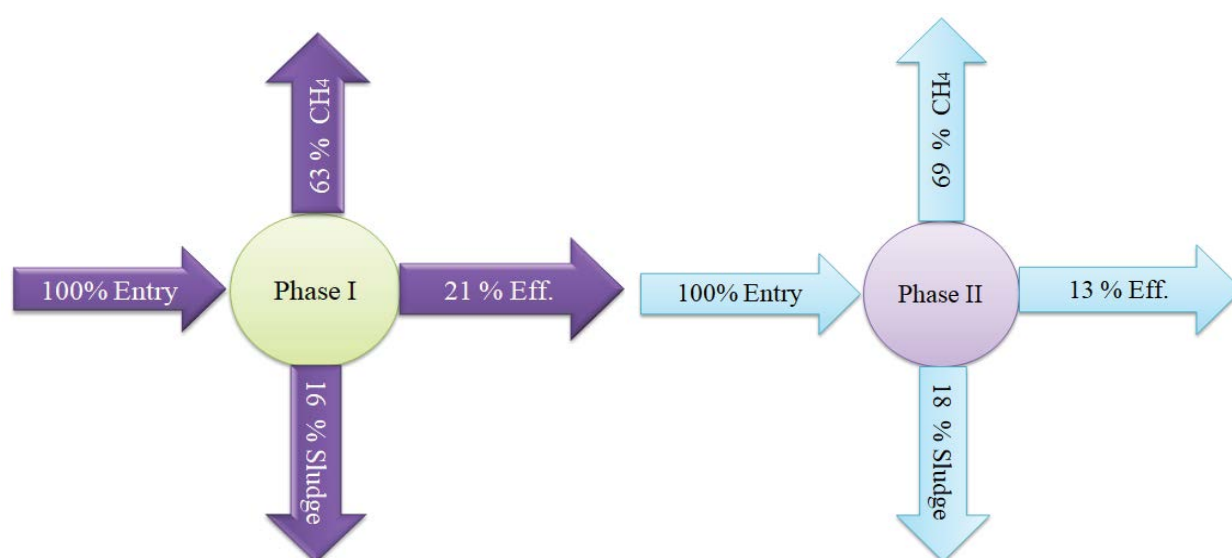
Fig. 8. Mass balance fraction behaviours of the carbonaceous material behavior for phases I and II.

obtained. Total phosphorus removal efficiencies were 15.4% and 17.7% for phases I and II, respectively. The removal of these nutrients was low, mainly due to their absorption by the biomass for its growth in the bioreactor and in the DM. Similar values were found by Wang et al. [51], Ershain et al. [56], and Ershain et al. [58].

3.5. Mathematical modeling for fouling mechanism in dynamic membrane formation

The mathematical modeling to evaluate better filtration adjustment over time is presented in Table 7, and the respective graphic representations are presented in Fig. 9 and Fig. S4.

The values presented in Table 7 indicate that the cake filtration model had the best fit (higher R^2_{adj} and lower RSS) with the experimental data than the other three blocking models in all phases, thus confirming the prominence of DM formation during filtration and high solid-liquid separation.

It is worth remembering that the cake filtration model has as a premise that the particles are larger than the support material pore size, and the particle concentration is high, therefore not blocking them. Higher adjustment efficiency of the DM in both phases can be explained by the high concentration of solids and the inoculum sludge's capability to be sedimented, which was in the range of 21 to 28.7 mg L⁻¹ of VSS, and 28.0 to 31.5 ml g⁻¹ of sludge volume index, respectively, as shown in Table 2. Pie et al. [59], with solids concentrations from 6 g L⁻¹ and a sludge index of 46 mL g⁻¹, observed excellent adsorption and filtration performance in a DM due to DM biomass increase, high EPS concentrations, and lower zeta potential levels, which provided agglomeration and flocculation of sludge, facilitating solid–liquid separation.

Similar results were obtained by Saleem et al. [24] in an AnDMBR system treating synthetic wastewater, under variations in TPM, concentration of solids, and support material pore sizes, in which the cake filtration model showed better adjustment to experimental data. The concentration of

Table 7
Mathematical modeling to evaluate DM mechanism formation in phases I and II

Experiment	Filtration model	Blocking constant	RSS	R^2_{adj}
Phase I	Complete blocking	2.858657332 1 s^{-1}	7,804.7371	0.80943
	Standard blocking	0.91149 1 m^{-3}	5,714.5691	0.92391
	Intermediate blocking	0.21114 1 m^{-3}	729.6441	0.93786
	Cake filtration	495167.04 s m^{-6}	90.23941	0.99912
Phase II	Complete blocking	0.394013276 1 s^{-1}	17,113.943	0.72969
	Standard blocking	0.80469 1 m^{-3}	13,963.394	0.82147
	Intermediate blocking	0.37696 1 m^{-3}	1,939.1860	0.92283
	Cake filtration	1510397.28 s m^{-6}	169.26459	0.99758

solids was unique, with significant influence in the adjustment of the respective model. They concluded that the cake filtration mechanism can be effectively used to explain the DM formation process.

They also inferred that, although the complete blocking model showed the lowest efficiency in adjusting the experimental data, R^2_{adj} often reached values greater than 0.90, demonstrating that it can reasonably describe the occurrence of fouling in DMs. Therefore, in the present study, for the complete blocking model, Table 7 shows that R^2_{adj} was less than 0.9 in the two phases. It is clearly observed, by Fig. 9 and S4, that the complete blocking model is extremely deviated to fit with experimental data.

Li et al. [25] also had large deviation for the complete blocking model (R^2_{adj} = 0.799) when testing the effects of different affluent flows on DM formation for treatment of synthetic wastewater in an AnDMBR. They also found the cake filtration model to be the best fit for experimental data in all tested flows (R^2_{adj} = 0.994). They concluded that with the knowledge of DM mechanism formation, through the equations of the theoretical model curve and the experimental data plotted, it is possible to predict the key control point and use it to optimize the operational strategy.

However, when comparing with other types of studies such as those of aerobic dynamic membrane bioreactors, a different scenario is observed. Li et al. [60] verified DM mechanism formation in different types of mesh support, with adjustment composed of three models, and divided into two stages of operation. The standard blocking model was the dominant mechanism during the initial filtration stage, and the complete blocking and cake filtration models dominated in the final stage of operation. Liu et al. [8] verified progressive DM development in silk mesh characterized by adjustment in all models, which occurred sequentially (complete blocking, standard blocking, intermediate blocking, and cake filtration).

Also looking at conventional MBRs, Vela et al. [61] investigated the fouling mechanisms for a UF process and concluded that the fouling mechanism was dependent on operating conditions such as TMP and tangential speed. Sampath et al. [62] investigated modeling in the MF membrane with different pore sizes, different depths, and constant TMP. The authors explained that none of the models individually provided a satisfactory fit with the experimental data, indicating that more than one fouling mechanism was present during system operation. Smaller

pore size membranes obtained adjustment for the full blocking model, followed by cake filtration. Larger pore size membranes obtained adjustment for the intermediate blocking model, followed by cake filtration.

Therefore, retrospectively, it is elucidated that the fouling mechanism for DM formation for the present study was predominated by cake filtration, with the main cause being the sludge concentration. This is in accordance with the studies done by other researchers using an AnDMBR system. While for DMBR and MBR systems, the fouling mechanism is generally predominated by, at least, two block models. These block models can be influenced by several factors such as TMP, tangential velocity, pore size, sludge particle diameter, sludge properties, and hydrodynamic conditions.

4. Conclusions

The DM was successfully generated under anaerobic conditions, under high initial permeate fluxes of 1,170 and 1,755 L m^{-2} h^{-1}, in a low-cost support mesh (polypropylene) with a pore diameter of 90 μm, at ambient temperature. However, for an initial permeate flux of 1,755 L m^{-2} h^{-1}, low stability was experienced, and TMP reached values greater than 40 kPa, thus causing DM layer dissociation and elution of biological flocs for effluent close to the end of operation.

The application of backwashing after a 10% reduction of the permeate flux allowed prolonged filtration under hydraulic pressure. For both permeate fluxes tested, the total resistance to filtration value was of 10^{11} m^{-1}, implying excellent filterability by the DM, and an energy saving potential for the AnDMBR system.

The AnDMBR performed well in domestic sewage treatment, achieving a VFA reduction between 48.4% and 57.3%, obtaining a total COD removal efficiency of 81% to 88%, soluble COD of 65% to 79%, and color of 63% to 80%. The removal of suspended solids achieved 94% efficiency, producing an effluent with low turbidity (17 NTU) which meets the WHO [63] recommendations of <1 helminth egg per liter for unrestricted irrigation.

Although the amount of biogas measured in the system was low, when compared to its theoretical value, the mass balance demonstrated that the COD fraction converted to methane was greater than 63%, ensuring a significant amount of biogas produced by the system. It is likely that
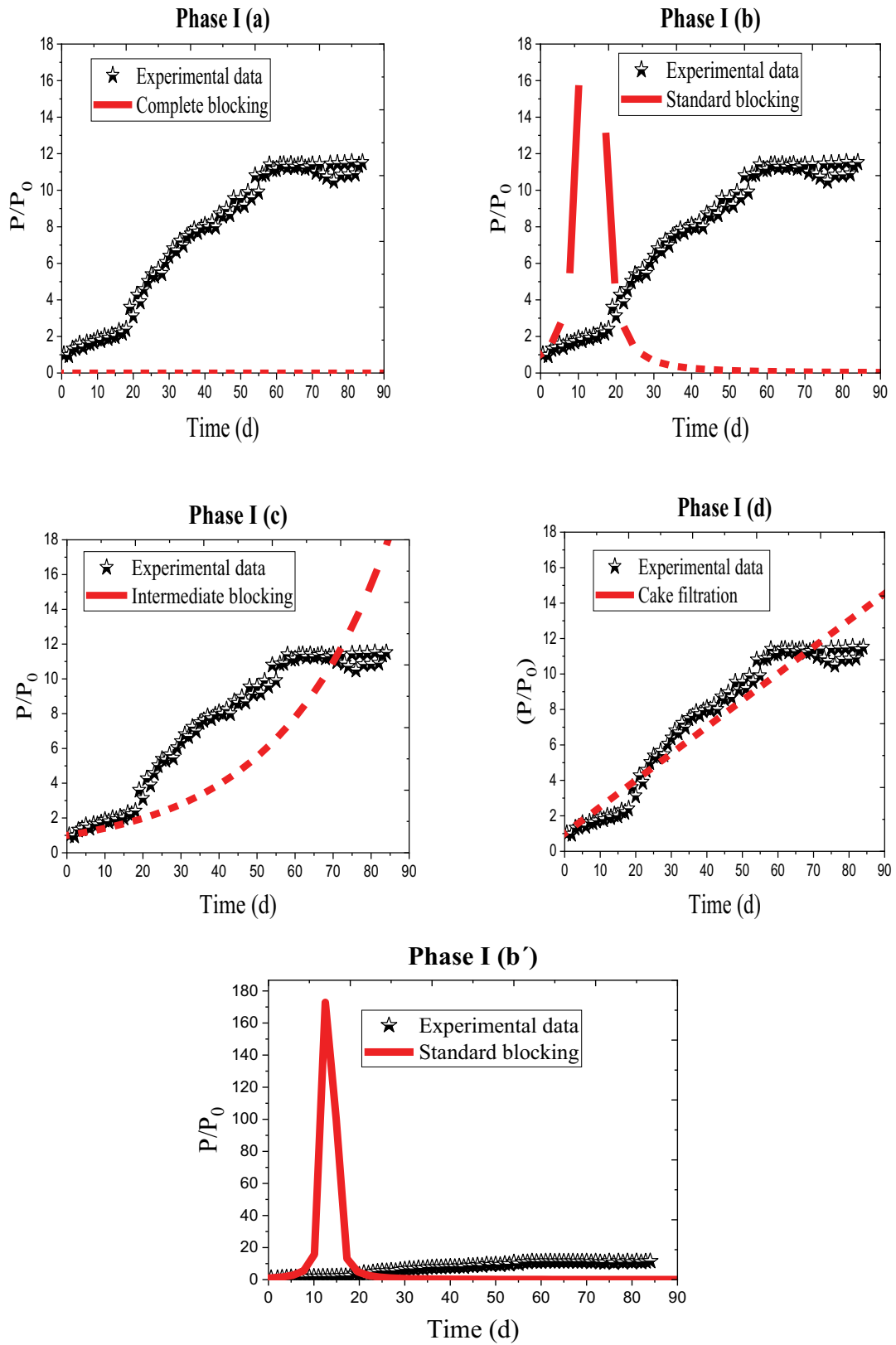
Fig. 9. Filtration model[1] curves for phase I.

most of it came out in dissolved form with the effluent due to supersaturation in the liquid medium.

The fouling mechanism predominant in DM formation in the two permeate fluxes tested was cake filtration, with the main cause being the concentration of inoculum sludge, thus explaining the high solid-liquid separation.

Acknowledgments

ORCID

Jacob Fortuna José Chimuca, https://orcid.org/0000-0001-7143-7443
José Tavares de Sousa: http://orcid.org/0000-0002-1056-1771
Wilton Silva Lopes: http://orcid.org/0000-0002-0151-7664
Catarina Simone Andrade do Canto: https://orcid.org/0000-0002-6078-8560
Valderi Duarte Leite: http://orcid.org/0000-0001-5861-7407

References

[1] S. Judd, The MBR Book: Principles and Applications of Membrane Bioreactors for Water and Wastewater Treatment, 1st ed., Butterworth-Heinemann, Oxford, 2006.

[2] S. Judd, The status of membrane bioreactor technology, Trends Biotechnol., 26 (2011) 109–116.

[3] X. Du, Y. Shi, V. Jegatheesan, I. Ul Haq, A review on the mechanism, impacts and control methods of membrane fouling in MBR system, Membranes, 10 (2020) 1–33.

[4] A. Foglia, Ç. Akyol, N. Frison, E. Katsou, A.L. Eusebi, F. Fatone, Long-term operation of a pilot-scale anaerobic membrane bioreactor (AnMBR) treating high salinity low loaded municipal wastewater in real environment, Sep. Purif. Technol., 236 (2020)1–11.

[5] P. Vergine, C. Salerno, G. Berardi, A. Pollice, Self-Forming Dynamic Membrane BioReactors (SFD MBR) for municipal wastewater treatment: relevance of solids retention time and biological process stability, Sep. Purif. Technol., 255 (2021) 1–8.

[6] F. Zhang, W. Jing, W. Xing, N. Xu, Experiment and calculation of filtration processes in an external-loop airlift ceramic membrane bioreactor, Chem. Eng. Sci., 64 (2009) 2859–2865.

[7] Q. Zhao, Q. An, Y. Ji, J. Quian, C. Gao, Polyelectrolyte complex membranes for pervaporation, nanofiltration and fuel cell applications, J. Membr. Sci., 379 (2011) 19–45.

[8] H. Liu, C. Yang, W. Pu, J. Zhang, Formation mechanism and structure of dynamic membrane in the dynamic membrane bioreactor, Chem. Eng. J., 148 (2009) 290–295.

[9] O. Isik, R. Hudayarizka, A. Abdelrahman, H. Ozgun, M. Ersahin, I. Demira, I. Koyuncu, Impact of support material type on performance of dynamic membrane bioreactors treating municipal wastewater, J. Chem. Technol. Biotechnol., 95 (2020) 2437–2446.

[10] G. Amy, Fundamental uderstanding of organic matter foulling of membranes, Desalination, 231 (2008) 44–51.

[11] Y. Yang, Y. Zang, Y. Hu, X. Wang, H. Ngo, Upflow anaerobic dynamic membrane bioreactor (AnDMBR) for wastewater treatment at room temperature and short HRTs: process characteristics and practical applicability, Chem. Eng. J., 383 (2020) 1–10.

[12] M. Ersahin, H. Ozgun, R. Dereli, R. Ozturk, K. Roest, J. van Lier, A review on dynamic membrane filtration: Materials, applications and future perspectives, Bioresour. Technol., 122 (2012) 196–206.

[13] M. Siddiqui, J. Dai, Y. Luo, G. Chen, Investigation of the short-term effects of extracellular polymeric substance accumulation with different backwashing strategies in na anaerobic self-forming dynamic membrane bioreactor, Water Res., 185 (2020) 1–10.

[14] L. Alibardi, R. Cossu, M. Saleem, A. Spagni, Development and permeability of a dynamic membrane for anaerobic wastewater treatment, Bioresour. Technol., 161 (2014) 236–244.

[15] J. Wang, A. Cahyadi, B. Wu, W. Pee, A. Fane, J. Chew, The roles of particles in enhancing membrane filtration: a review, J. Membr. Sci., 595 (2020) 1–29.

[16] D. Guan, M. Siddiqui, G. Chen, Comparison of different chemical cleaning reagents on fouling recovery in a self-forming dynamic membrane bioreactor (SFDMBR), Sep. Purif. Technol., 206 (2018) 158–165.

[17] X. Zhang, Z. Wang, Z. Wu, F. Lu, J. Tong, L. Zang, Formation of dynamic membrane in an anaerobic membrane bioreactor for municipal wastewater treatment, Chem. Eng. J., 165 (2010) 175–183.

[18] M. Ersahin, Y. Tao, H. Ozgun, J. Gimenez, H. Spanjers, J. van Lier, Impact of anaerobic dynamic membrane bioreactor configuration on treatment and filterability performance, J. Membr. Sci., 526 (2017) 387–394.

[19] M. Siddiqui, J. Dai, D. Guan, G. Chen, Exploration of the formation of self-forming dynamic membrane in an upflow anaerobic sludge blanket reactor, Sep. Purif. Technol. 212 (2019) 757–766.

[20] J. Ma, Z. Wang, X. Zou, J. Feng, Z. Wu, Microbial communities in an anaerobic dynamic membrane bioreactor (AnDMBR) for municipal wastewater treatment: comparison of bulk sludge and cake layer, Process Biochem., 48 (2013) 510–516.

[21] Y. Hu, Y. Yang, Y. Zang, J. Zhang, X. Wang, Anaerobic Dynamic Membrane Bioreactors (AnDMBRs) for Wastewater Treatment, In: Current Development in Biotechnology and Bioengineering, Elsevier, Xi'an, 2020, pp. 260–277.

[22] Y. Liu, H. Liu, L. Cui, K. Zhang, The ration of food-to-microorganism (F/M) on membrane fouling of anaerobic membrane bioreactors treating low-strength wastewater, Desalination, 297 (2012) 97–103.

[23] F. Meng, Y. Zhang, Z. Oh, H. Zhou, S. Shin, Fouling in membrane bioreactors: an updated review, Water Res., 114 (2017) 151–180.

[24] M. Saleem, L. Alibardi, R. Cossu, M. Lavagnolo, A. Spagni, Analysis of fouling development under dynamic membrane filtration operation, Chem. Eng. J., 312 (2017) 136–143.

[25] L. Li, G. Xu, H. Yu, J. Xing, Dynamic membrane for micro-particle removal in wastewater treatment: performance and influencing factors, Sci. Total Environ., 627 (2018) 332–340.

[26] E. Iritani, N. Katagiri, Developments of blocking filtration model in membrane filtration, Kona Powder Part. J., 33 (2016) 179–202.

[27] Metcalf & Eddy, Waste Engineering: Treatment and Reuse, 4th ed., New York, 2003.

[28] J.F.J. Chimuca, T.J. Sousa, W.S. Lopes, V.D. Leite, C.S.A. Canto, Decentralized treatment of domestic sewage in dynamic membrane bioreactor, Desal. Water Treat., 197 (2020) 76–89.

[29] R. Ramos, T. Albuquerque, W. Lopes, Sistema de monitoramento on-line de biorreatores (SISMOBIO), Titular: Universidade Estadual da Paraíba-UEPB, BR n. 512020002858–6, Depósito: 15 dez. 2020, Concessão: 22 dez.

[30] A. van Haandel, G. Lettinga, Tratamento Anaeróbio de Esgotos: Um Manual para Regiões de Clima Quente, Campina Grande, 1994.

[31] C.A.L. Chernicharo, Reatores Anaeróbios: Princípios do Tratamento Biológico de Águas Residuárias, secunda ed., Belo Horizonte, 2007.

[32] Y. Hu, Y. Yang. S. Yu, X.C. Wang, J. Tang, Psychrophilic anaerobic dynamic membrane bioreactor for domestic wastewater treatment: effects of organic loading and sludge recycling, Bioresour. Technol., 270 (2018) 62–69.

[33] APHA, Standard Methods for Examination of Water and Wastewater, 22nd ed., American Public Health Association, Washington, DC, 2012.

[34] WHO, Analysis of Wastewater for Use in Agriculture, Laboratory Manual of Parasitological and Bacteriological Techniques, World Health Organization, Geneva, 1996.

[35] B. Frøund, R. Palmgren, K. Keiding, P. Nielsen, Extraction of extracellular polymers from activated sludge using a cation exchange resin, Water Res., 30 (1996) 1749–1758.

[36] M. Dubois, K. Gilles, J. Hamilton, P. Rebers, F. Smith, Colorimetric method for determination of sugars and related substances, Anal. Chem., 28 (1956) 350–356.

[37] D. Guan, J. Dai, Y. Watanabe, G. Chen, Changes in the physical properties of the dynamic layer and its correlation with permeate quality in a self-forming dynamic membrane bioreactor, Water Res., 140 (2018b) 67–76.

[38] M. Ersahin, Y. Tao, H. Ozgun, H. Spanjers, J. van Lier, Characteristics and role of dynamic membrane layer in anaerobic membrane bioreactors, Biotechnol. Bioeng., 113 (2016) 761–771.

[39] Y. Shi, J. Huang, G. Zeng, Y. Gu, B. Tang, J. Zhou, Y. Yang, L. Shi, Evaluation of soluble microbial products (SMP) on membrane fouling in membrane bioreactors (MBRS) at the fractional and overall level: a review, Rev. Environ. Sci. Biotechnol., 17 (2018) 71–85.

[40] F. Sun, N. Zhang, F. Lib, X. Wang, J. Zhang, L. Song, S. Liang, Dynamic analysis of self-forming dynamic membrane (SFDM) filtration in submerged anaerobic bioreactor: performance, characteristic, and mechanism, Bioresour. Technol., 270 (2018) 383–390.

[41] H. Lin, K. Xie, B. Mahendran, K. Leung, S. Liss, B. Liao, Sludge properties and their effects on membrane fouling in submerged anaerobic membrane bioreactors (SAnMBRs), Water Res., 43 (2009) 3827–3837.

[42] L. Hao, S. Liss, B. Liao, Influence of COD: N ratio on sludge properties and their role in membrane fouling of a submerged membrane bioreactor, Water Res., 89 (2016) 132–141.

[43] Y. Zhu, L. Cao, L. Ni, Y. Wang, Insights into fouling behavior in a novel anammox self-forming dynamic membrane bioreactor by the fluorescence EEM-PARAFAC analysis, Environ. Sci. Pollut. Res., 27 (2020) 40041–40053.

[44] H. Liu, L. Wang, X. Zhang, B. Fu, B. Liu, Y. Li, X. Lu, A viable approach for commercial VFAs production from sludge: liquid fermentation in anaerobic dynamic membrane reactor, J. Hazard. Mater., 365 (2019) 912–920.

[45] Y. Hu, X. Wang, Q. Sun, H. Ngo, Z. Yu, J. Tang, Characterization of a hybrid powdered activated carbon-dynamic membrane bioreactor (PAC-DMBR) process with high flux by gravity flow: operational performance and sludge properties, Bioresour. Technol., 223 (2017) 65–73.

[46] Z. Yu, Y. Hu, M. Dzakpasu, X. Wang, Thermodynamic prediction and experimental investigation of short-term dynamic membrane formation in dynamic membrane bioreactors: effects of sludge properties, J. Environ. Sci., 77 (2019) 85–96.

[47] L. Alibardi, N. Bernava, R. Cossu, A. Spagni, Anaerobic dynamic membrane bioreactor for wastewater treatment at ambient temperature, Chem. Eng. J., 284 (2016)130–138.

[48] A. Pollice, P. Vergine, Chapter 10 – Self-Forming Dynamic Membrane Bioreactors (SFD MBR) for Wastewater Treatment: Principles and Applications, In: Current Development in Biotechnology and Bioengineering Advanced Membrane Separation Processes for Sustainable Water and Wastewater Management – Case Studies and Sustainability Analysis, Elsevier, Bari, 2020, pp. 235–258.

[49] H. Liu, Y. Wang, B. Yin, Y. Zhu, B. Fu, H. Liu, Improving volatile fatty acid yield from sludge anaerobic fermentation through self-forming dynamic membrane separation, Bioresour. Technol., 218 (2016) 92–100.

[50] M. Paçal, N. Semerci, B. Çall, Treatment of synthetic wastewater and cheese whey by the anaerobic dynamic membrane bioreactor, Environ. Sci. Pollut. Res. Int., 26 (2019) 32942–32956.

[51] L. Wang, H. Liu, W. Zhang, T. Yu, Q. Jin, B. Fu, H. Liu, Recovery of organic matters in wastewater by self-forming dynamic membrane bioreactor: performance and membrane fouling, Chemosphere, 203 (2018) 123–131.

[52] Y. Berkessa, B. Yan, T. Li, V. Jegatheesan, Y. Zhang, Treatment of anthraquinone dye textile wastewater using anaerobic dynamic membrane bioreactor: performance and microbial dynamics, Chemosphere, 238 (2020) 1–11.

[53] Z. Yu, Y. Hu, M. Dzakpasu, X. Wang, H. Ngo, Dynamic membrane bioreactor performance enhancement by powdered activated carbon addition: evaluation of sludge morphological, aggregative and microbial properties, J. Environ. Sci., 75 (2019) 73–83.

[54] A. Pauss, G. Andre, M. Perrier, S. Guiot, Liquid-to-gas mass transfer in anaerobic processes: inevitable transfer limitations of methane and hydrogen in the biomethanation process, Appl. Environ. Microbiol., 56 (1990) 1636–1644.

[55] Y. Hu, X. Wang, H. Ngo, Q. Sun, Y. Yang, Anaerobic dynamic membrane bioreactor (AnDMBR) for wastewater treatment: a review, Bioresour. Technol., 247 (2018) 1107–1117.

[56] M. Ersahin, J. Gimenez, H. Ozgun, Y. Tao, H. Spanjers, J. van Lier, Gas-lift anaerobic dynamic membrane bioreactors for high strength synthetic wastewater treatment: effect of biogas sparging velocity and HRT on treatment performance, Chem. Eng. J., 305 (2016) 46–53.

[57] J.B. van Lier, N. Mahmoud, G. Zeeman, Anaerobic Wastewater Treatment, In: Biological Wastewater Treatment: Principles, Modelling and Design, IWA Publishing, London, UK, 2008, pp. 401–442.

[58] M. Ersahin, H. Ozgun, Y. Tao, J. van Lier, Applicability of dynamic membrane technology in anaerobic membrane bioreactor, Water Res., 48 (2014) 420–429.

[59] Q. Pei, J. Luo, M. Chen, Studies on a new stainless steel mesh dynamic membrane for wastewater treatment, Bioresour. Technol., 297 (2020) 1–8.

[60] W. Li, G. Sheng, Y. Wang, X. Liu, J. Xu, H. Yu, Filtration behaviors and biocake formation mechanism of mesh filters used in membrane bioreactors, Sep. Purif. Technol., 81 (2011) 472–479.

[61] M. Vela, A. Blanco, J. García, B. Rodrígue, Analysis of membrane pore blocking models adapted to crossflow ultrafiltration in the ultrafiltration of PEG, Chem. Eng. J., 149 (2009) 232–241.

[62] M. Sampath, A. Shukla, A. Rathore, Modeling of filtration processes—microfiltration and depth filtration for harvest of a therapeutic protein expressed in *Pichia pastoris* at constant pressure, Bioengineering, 1 (2014) 260–277.

[63] WHO, Guidelines for the Safe Use of Wastewater, Excreta and Greywater, Vol. 2, Wastewater Use in Agriculture, World Health Organization, Geneva, 2006.

Supporting information

Table S1
AnDMBR system dimensions

Anaerobic bioreactor	Membrane module	Operation parameters
A_2 = 314 cm²	D_m = 7 cm	HRT = 8 h
V_2 = 62.8 L	A_m = 38.465 cm²	Phase I CRT = 84 d
V_u = 53.4 L	M_p: 90 μm	Q_e = 6.75 L h⁻¹
V_z = 9.42 L		J_P = 1,754.8 L m⁻² h⁻¹
		OLR = 2.90 kg COD m⁻³ d⁻¹
		v = 0.215 m s⁻¹
		HRT = 12 h
		Phase II CRT = 76 d
		Q_e = 4.5 L h⁻¹
		J_P = 1,754.8 L m⁻² h⁻¹
		OLR = 1.87 kg COD m⁻³ d⁻¹
		v = 0.143 m s⁻¹

A_2: bioreactor area; V_2: total bioreactor volume; V_u: useful bioreactor volume; V_z: headspace volume; D_m: inner membrane module diameter; A_m: membrane module useful area; Q_e: influent feed flow into the system; J_P: permeate flux; CRT: cell retention time; M_p: support mesh medium pore size; OLR: organic loading rate; v: surface velocity.
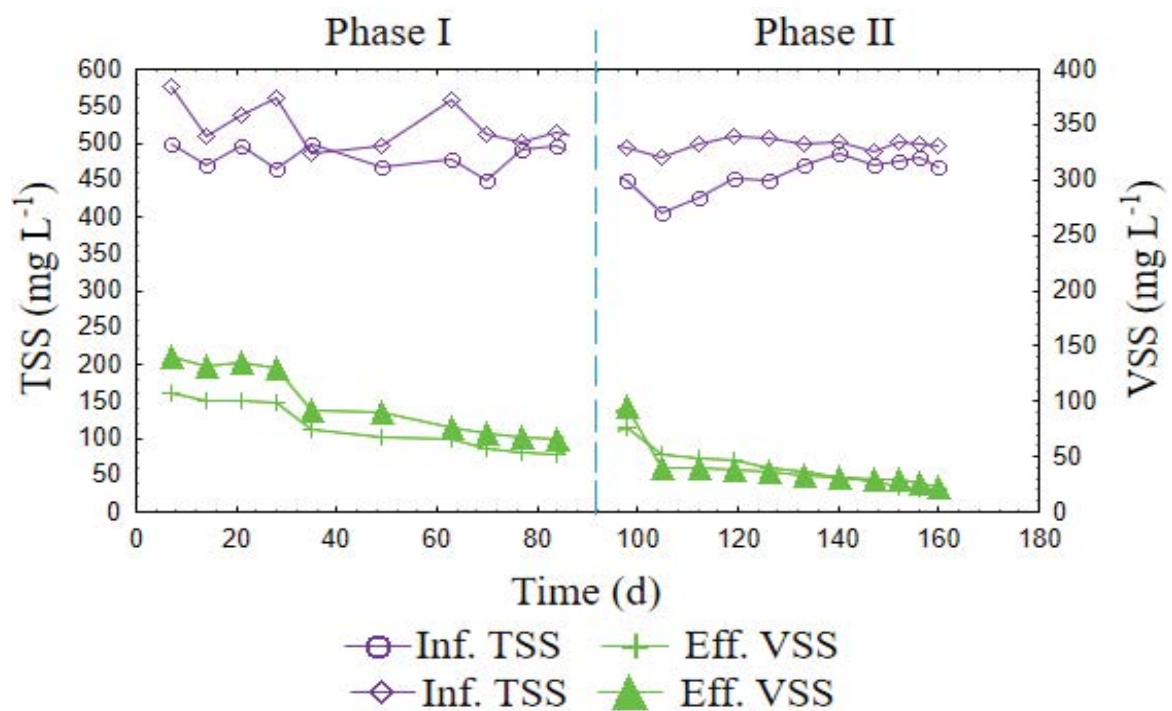

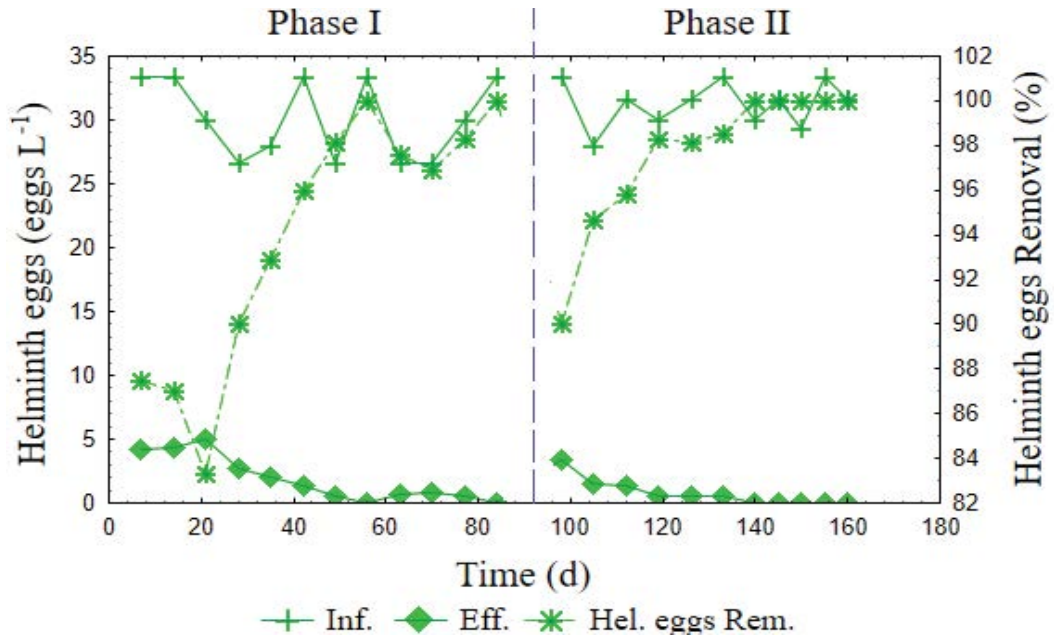Fig. S1. Solid fraction average values during phases I and II of operation.

Fig. S2. Helminth eggs average values in phases I and II.

Table S2
Helminth eggs frequency in stages I and II

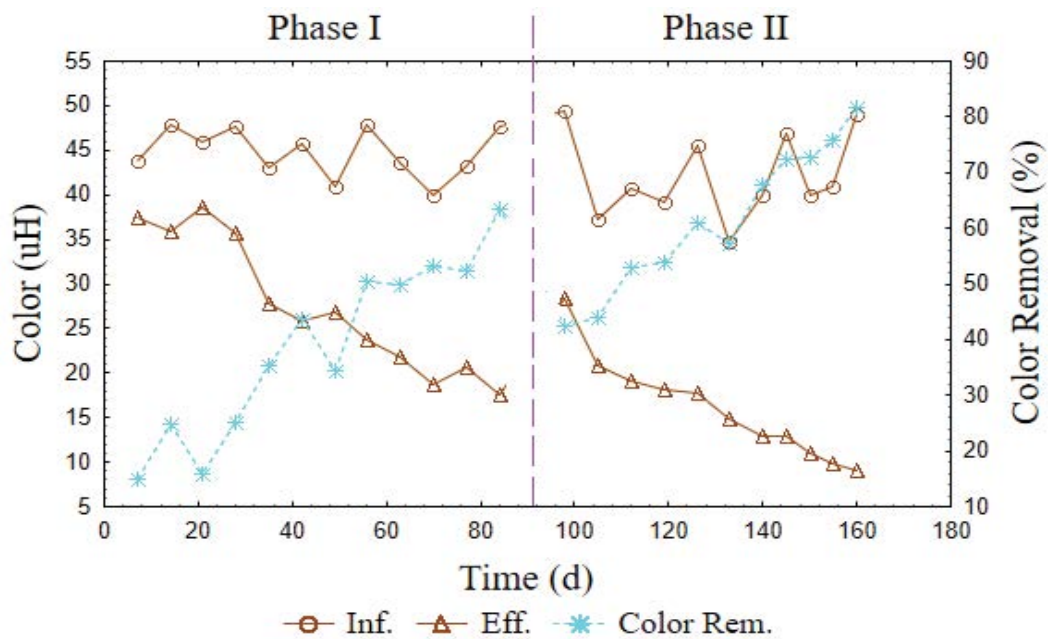| Helminth eggs	Phase I		Phase II	
	Inf.	Eff.	Inf.	Eff.
Ascaris lumbricoides (%)	62.5	62.1	67.3	53.9
Hookworms (%)	17.9	17.2	15.4	23.1
Enterobius sp. (%)	12.5	13.8	13.5	15.4
Hymenolepis sp. (%)	7.1	6.9	3.8	7.7

Fig. S3. Color variation during operation time in phases I and II.

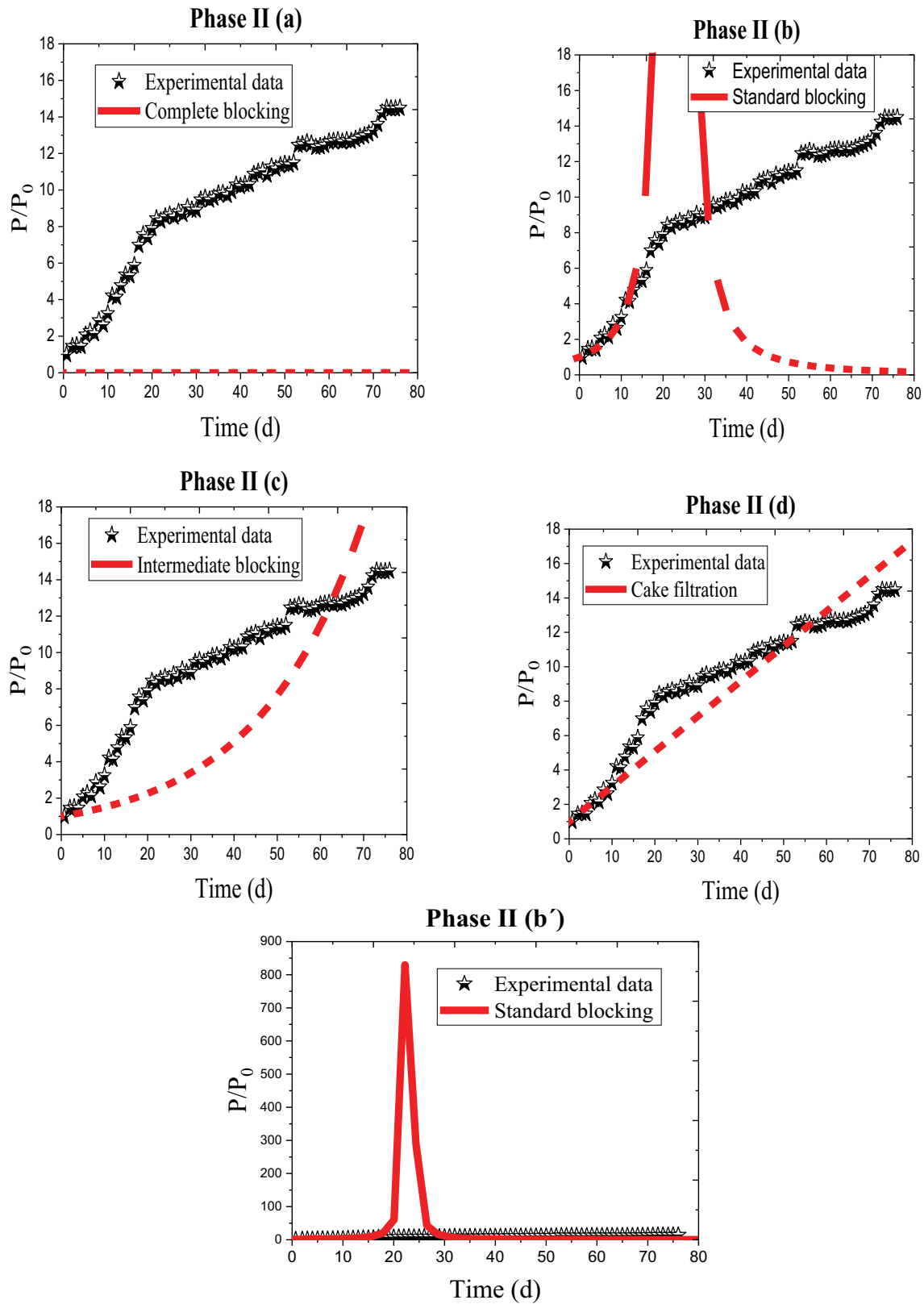Fig. S4. Filtration[1] curve models for phase II.

---

[1]'b′' indicates the original scale provided by the model in the Origin Pro 18 software.